Butyryl/Caproyl-CoA:Acetate CoA-Transferase: Cloning, Expression and Characterization of the Key Enzyme Involved in Medium-Chain Fatty Acid Biosynthesis

Qingzhuoma Yang[a,b], Shengtao Guo[b,c], Qi Lu[a,b], Yong Tao[a,d,#], Decong Zheng[a,b], Qinmao Zhou[a,b], Jun Liu[d]

[a] Key Laboratory of Environmental and Applied Microbiology, Environmental Microbiology Key Laboratory of Sichuan Province, Chengdu Institute of Biology, Chinese Academy of Science, Chengdu 610041, China

[b] University of Chinese Academy of Sciences, Beijing 100049, China

[c] BGI Education Center, University of Chinese Academy of Sciences, Shenzhen 518083, China

[d] Faculty of Bioengineering, Sichuan University of Science & Engineering, Xueyuan Street 180[#], Huixing Rd. 643000, Zigong, P.R. China

To whom correspondence should be addressed. Email: taoyong@cib.ac.cn.

Running title: Caproyl-CoA:Acetate CoA-Transferase

Keywords: CoA-transferase, chain elongation, Medium-chain Fatty Acids, *Ruminococcaceae* bacterium, Caproic acid

Abstract

Coenzyme A transferases (CoATs) are important enzymes involved in carbon chain elongation contributing to medium-chain fatty acid (MCFA) biosynthesis. For example, butyryl-CoA:acetate CoA transferase (BCoAT) is responsible for the final step of butyrate synthesis from butyryl-CoA. However, little is known about caproyl-CoA:acetate CoA-transferase (CCoAT), which is responsible for the final step of caproate synthesis from caproyl-CoA. In this study, two CoAT genes from *Ruminococcaceae* bacterium CPB6 and *Clostridium tyrobutyricum* BEY8 were identified by gene cloning and expression analysis. The enzyme assays and kinetic studies were carried out using butyryl-CoA or caproyl-CoA as the substrate. CPB6-CoAT can catalyze the conversion of both butyryl-CoA to butyrate and caproyl-CoA to caproate, but its catalytic efficiency with caproyl-CoA as the substrate was 3.8 times higher than that with butyryl-CoA. In contrast, BEY8-CoAT had only BCoAT activity, not CCoAT activity. This demonstrated the existence of a specific CCoAT involved in chain elongation via the reverse β-oxidation pathway. Comparative bioinformatics analysis showed the presence of a highly conserved motif (GGQXDFXXGAXX) in CoATs, which is predicted to be the active center of CoATs. Single point mutations in the conserved motif of CPB6-CoAT (Asp346 and Ala351) led to marked decreases in the activity for butyryl-CoA and caproyl-CoA, indicating that the conserved motif is the active center of CPB6-CoAT, and sites Asp346 and Ala351 were critical residues that affect enzymatic activity. This work provides insight into the function of CCoAT in caproic acid biosynthesis and improves the understanding of the chain elongation pathway for MCFA production.

Introduction

Medium-chain fatty acids (MCFAs, C6-C12) are widely utilized in agriculture and industry. For example, *n*-caproic acid (C6) is used as a precursor for the production of fragrances (1), antimicrobial agents (2), and drop-in biofuels (3). Recent studies have shown that MCFAs produced from renewable feedstock by anaerobic fermentation hold promise for replacing fossil resources and botanical oils such as palm kernel oil to meet the requirements for sustainable development (4). A few microorganisms, such as *Megasphaera elsdenii* (5), *Ruminococcaceae* bacterium CPB6 (6), *Acinetobacter* spp. (7), and *Clostridium kluyveri* (8), have been reported to be able to synthesize MCFAs from renewable feedstock via the carbon chain elongation pathway (9). In the process of chain elongation, intermediates of acidogenesis, such as acetate (C2) and *n*-butyrate (C4), as substrates are elongated to caproic acid (C6) and octanoic acid (C8) by adding acetyl-CoA in reverse β-oxidation cycles (10,11). C2 or C4, transformed to acetyl-CoA or butyryl-CoA, respectively, represents the initial substrate for elongation in reverse β-oxidation. The pathway has been identified as a key metabolic process in MCFA biosynthesis (12).

The production of high concentrations of butyrate (>10 mM) in vitro has been reported in some anaerobes, such as *Roseburia* (13) and *Faecalibacterium* (14). Butyrate is normally generated from two molecules of acetyl-CoA, yielding acetoacetyl-CoA, which is then converted to butyryl-CoA (15). In the latter reaction, butyryl-CoA is exchanged with exogenously derived acetate to yield acetyl-CoA and butyrate (16). The enzymes responsible for butyrate production in the reverse β-oxidation pathway comprise acetyl-CoA acetyltransferase (AtoB), 3-hydroxybutyryl-CoA dehydrogenase (Hbd), enoyl-CoA hydratase (Crt), butyryl-CoA dehydrogenase (Bcd), and butyryl-CoA:acetate CoA-transferase (BCoAT) (17). Among them, BCoAT is a well-known CoA-transferase (CoAT) responsible for the final step of butyric acid synthesis, transforming the CoA moiety from butyryl-CoA to an exogenous acetate molecule, which results in the formation of butyrate and acetyl-CoA (18,19). CoATs are abundant in anaerobic fermenting bacteria that cope

with low ATP yields, but they are also found in aerobic bacteria and in the mitochondria of humans and other mammals (20). The synthesis pathway and key genes associated with butyric acid in MCFA biosynthesis via reverse β-oxidation are well understood. However, little is known about key genes involved in the conversion of butyric acid (C4) to caproic acid (C6). Although most genes responsible for butyric acid production are suggested to function in further chain elongation of MCFAs (17), the fact that many butyrate-producing bacteria, such as *Clostridium tyrobutyricum,* produce only butyric acid instead of caproic acid via the reverse β-oxidation pathway suggests that there may be different functional genes involved in the production of caproic acid.

Recently, our study showed that *Ruminococcaceae* bacterium CPB6 is a caproic acid-producing bacterium with the highly prolific ability to perform chain elongation and can produce caproic acid (C6) from lactate (as an electron donor) with C2-C4 carboxylic acids and heptoic acid (C7) with C3-C5 carboxylic acids as electron acceptors (EAs) (21,22). Moreover, a set of genes correlated with chain elongation were identified by sequencing and annotating the whole genome of the CPB6 strain (23). However, very little information is available on enzymes involved in the conversion of C4 to C6, especially the gene responsible for the conversion of caproyl-CoA to caproic acid.

In this study, we cloned a predicted CCoAT gene from the caproic acid-producing strain CPB6 (21) and a BCoAT gene from the butyric acid-producing *C. tyrobutyricum* BEY8 (24) and expressed the two proteins in *Escherichia coli* BL21 (DE3) with the plasmid pET28a. The aims of this study were to (i) compare differences in sequence, structure, enzymatic activity and substrate specificity between the CCoAT and BCoAT; (ii) identify the active center of the CCoAT and its effects on the activities of enzymes with different structures; and (iii) verify the existence of the CCoAT in the caproic acid biosynthesis pathway.

Results and Discussion

Cloning, expression, and purification of CoA-transferase

According to the genome sequences of strains CPB6 and *C. tyrobutyricum* BEY8, specific primers targeting CoAT genes were designed and synthesized (Table 1). Agarose gel electrophoresis showed that the size of the PCR products and the double-digestion products was approximately 1300 bp, consistent with the expected sizes of CPB6-CoAT (1344 bp) (Fig. S1) and the BEY8-CoAT gene (1233 bp) (Fig. S2). Sequence analysis of the recombinant CoAT plasmids showed that the cloned genes shared 100% similarity with the predicted CoAT genes of strains CPB6 (CCoAT) and BEY8 (BCoAT). This finding indicated that the recombinant *E. coli*/pET28a-CCoAT and *E. coli*/pET28a-BCoAT were successfully constructed.

To characterize the functions of CoAT proteins, the two recombinant plasmids (pET28a-CCoAT and pET28a-BCoAT) were expressed in *E. coli* BL21 (DE3). Single bands of the purified proteins were detected on SDS-polyacrylamide gels after affinity chromatography (Fig. 1*A*). As shown in Fig. 1*A*, there was no obvious protein band of approximately the size of the target protein in *E. coli*/pET28a (control), while a single band was observed in *E. coli*/pET28a-BCoAT (lane 2) and *E. coli*/pET28a-CCoAT (lane 3), and their sizes were consistent with the expected sizes of BEY8-CoAT (46 kDa) and CPB6-CoAT (49 kDa). Furthermore, western blotting analysis with a His-antibody (Fig. 1*B*) also demonstrated that the observed bands were consistent with the expected molecular mass of BEY8-CoAT and CPB6-CoAT (approximately 46-49 kDa).

Enzyme assay

The CoAT activity of crude enzyme extracts was determined by measuring the production of acetyl-CoA from butyryl-CoA or caproyl-CoA (25). It has been previously reported that the key reactions

for butyrate and caproate production were (1) butyryl-CoA + acetate→ butyrate + acetyl-CoA and (2) caproyl-CoA + acetate → caproate + acetyl-CoA (10,21,26). As shown in Table 2, the crude and purified BEY8-CoAT activities with butyryl-CoA and sodium acetate as substrates were 6.91±0.12 and 26.2±0.09 U/mg of protein, respectively. However, this enzyme showed no activity for caproyl-CoA. This result suggested that BEY8-CoAT is a BCoAT, similar to the CoAT from *Clostridium acetobutylicum* ATCC 824 that is able to produce butyrate instead of caproate, and its purified enzyme activity was 29.1 U/mg of protein (27). Moreover, the butyrate-producing bacterium *Coprococcus* sp. strain L2-50 from the human large intestine showed very high BCoAT activity (118.39±5.02 U/mg of protein) but no CCoAT activity (13). This result indicated that the BCoAT probably has substrate specificity for butyryl-CoA (29). In contrast, the activities of crude and purified CPB6-CoAT with butyryl-CoA and sodium acetate as substrates were 2.07±0.06 and 10.8 ±0.02 U/mg of protein, and the activities with caproyl-CoA and sodium acetate as substrates were 5.11±0.08 and 27.6±0.15 U/mg of protein, respectively (Table 2), indicating that CPB6-CoAT can catalyze the conversion of both butyryl-CoA to butyrate and caproyl-CoA to caproate. It is worth noting that the crude and purified CPB6-CoAT activity for caproyl-CoA was 2.5-2.6 times higher (5.11 vs 2.07, 27.56 vs 10.28 U/mg of protein) than that for butyryl-CoA, suggesting that CPB6-CoAT specifically prefers caproyl-CoA as a substrate instead of butyryl-CoA.

The BCoAT is required for butyrate biosynthesis in *Clostridium kluyveri* (13) and *C. tyrobutyricum* (28). This enzyme is responsible for the final step of butyrate production, catalyzing the conversion of butyryl-CoA and acetate to butyrate and releasing acetyl-CoA (16). As reported in previous studies, this enzyme is considered to be a biomarker for identifying butyrate-producing bacteria (16,27,29). However, BCoAT is not responsible for chain elongation of larger or higher-carbon-numbered (>C5) fatty acids (28). Seedorf et al.(17) speculated that BCoAT may catalyze the conversion of caproyl-CoA to caproate, similar to the conversion of butyryl-CoA to butyrate, based

on genome analysis of *C. kluyveri*, but no further research has been reported. Our previous study showed that the rate of caproate production with caproyl-CoA as the substrate in strain CPB6 was 3.5 times higher than that observed with butyryl-CoA as the substrate and suggested the existence of a CCoAT that specifically prefers caproyl-CoA instead of butyryl-CoA as the substrate (21). In this study, CPB6-CoAT was confirmed for the first time to be a CCoAT responsible for the final step of caproate formation, although it harbored low BCoAT activity for butyryl-CoA. These data demonstrated the existence of a specific CCoAT involved in the chain elongation of MCFAs, which is significantly different from the function of BCoAT. The detailed mechanism underlying this functional difference needs to be further studied.

Kinetics of CoA-transferases

The kinetic parameters of the recombinant proteins were investigated using a colorimetric assay according to a previous study (16). Initial velocities were determined at fixed sodium acetate concentrations with different butyryl-CoA or caproyl-CoA concentrations. K_m and V_m values were estimated from secondary plots (Materials and Methods). Additionally, k_{cat} values were calculated from enzyme concentrations in the reaction mixtures. The double-reciprocal plotting of enzyme kinetics showed that the reactions of the two CoATs follow the ternary-complex mechanism (Fig. S3), the result suggested that the CoATs of the CBP6 and BEY8 probably belong to family III, which can be distinguished kinetically(18).

As k_{cat}/K_m can be used to compare the catalytic efficiency of different substrates catalyzed by the same enzyme (30), a lower K_m value indicates that the enzyme has a higher affinity for the substrate and vice versa (31). In this study, the Km, k_{cat}, k_{cat}/K_m and V_m values of CPB6-CoAT with caproyl-CoA were 358.8 μM, 14.74 min^{-1}, 41.08 $mM^{-1}min^{-1}$ and 29.51 μM min^{-1}, respectively, and those with butyryl-CoA were 536.9 μM, 5.810 min^{-1}, 10.82 $mM^{-1}min^{-1}$ and 11.62 μM min^{-1}, respectively

(Table 3). The catalytic efficiency of CPB6-CoAT for caproyl-CoA was 3.8 times (41.08 vs 10.82 $mM^{-1}min^{-1}$) higher than that for butyryl-CoA, consistent with our previous result showing that the CCoAT activity is predominantly higher than the BCoAT activity (21). The K_m of CPB6-CoAT for caproyl-CoA was significantly lower than that for butyryl-CoA (358.8 vs 536.9 μM), exhibiting the higher affinity of this enzyme for caproyl-CoA relative to butyryl-CoA. These results also partly explained why caproate instead of butyrate is always the predominant product in the fermentation broth of strain CPB6 (22,23). BEY8-CoAT had only BCoAT activity, with K_m, *k*cat, k_{cat}/K_m and V_m values of 369.5 μM, 13.91 min^{-1}, 37.65 $mM^{-1}min^{-1}$ and 27.81 μM min^{-1}, respectively, and there was no detectable CCoAT activity (Tables 2 and 3), supporting our previous results showing that strain BEY8 produces only butyric acid as the predominant product (24). Similar to the results of Lee et al., the CoAT from *C. tyrobutyricum* only catalyzes the conversion of butyryl-CoA to butyrate and is not responsible for chain elongation of larger or higher-carbon-numbered (>C5) fatty acids (29).

The K_m of BEY8-CoAT for butyryl-CoA (369.5 μM) was obviously greater than that of CPB6-CoAT (536.9 μM), indicating that BEY8-CoAT had higher enzymatic affinity for butyryl-CoA than CPB6-CoAT. Similarly, CoAT (PGN_0725) from *Porphyromonas gingivalis* (15,16) and CoAT from *C. acetobutylicum* ATCC 824 (27) both catalyze the conversion of butyryl-CoA to butyrate, with K_m values of 520 μM and 21.01 μM, respectively. This indicated that the BCoAT generally had higher affinity and catalytic activity for butyryl-CoA than the CCoAT, while no BCoAT from butyric acid-bacteria displayed affinity and catalytic activity for caproyl-CoA. These results suggested that the BCoAT is only involved in chain elongation of C2 to C4, not in that of C4 to C6 or C8.

Phylogenetics of the whole genome and multiple amino acid sequence alignment

The whole-genome phylogenetic tree was constructed based on 119 single-copy genes (including CoATs) that were common among 29 strains (Fig. 2). These strains have a wide range of butyrate metabolic pathways (29), for example, *Roseburia* sp., *Faecalibacterium prausnitzii*, and *Coprococcus* sp. from the human gut exhibit BCoAT activity values of 38.95, 18.64 and 118.39 U/mg of protein (crude extracts), respectively (13). The two species closest to strain CPB6 were *Pygmaiobacter massiliensis* (32) and *F. prausnitzii* (33), which are also butyric acid-producing bacteria in human feces. Interestingly, the species closest to *C. tyrobutyricum* BEY8 was *C. kluyveri*, which is a well-known caproic acid-producing bacterium. This close relationship may be because they belong to the same genus, *Clostridium*.

Based on the alignment results generated from CoAT protein sequences from six different species, 14 amino acids (GXGGQXDFXXGAXX, position 340-353) of the CoATs in all the microbes were highly conserved (except in *M. elsdenii*), and their secondary structures consisted of 17 α-helices and 21 β-sheets (Fig. 3). The sequence similarities between CPB6-CoAT and the analyzed CoATs were as follows: *C. kluyveri* (37.67%), *M. elsdenii* (10.27%), *C. tyrobutyricum* BEY8 (38.04%), *Lachnospiraceae* bacterium (60.59%), and *Anaerostipes hadrus* (58.52%). Among the six bacteria, strain CPB6, *C. kluyveri*, and *M. elsdenii* are caproic acid-producing bacteria, while *C. tyrobutyricum* BEY8, *Lachnospiraceae* bacterium, and *A. hadrus* are butyric acid-producing bacteria. The alignment results showed that CPB6-CoAT shared lower similarity (10.27-37.67%) with the CoATs of *C. kluyveri* and *M. elsdenii* but higher similarity (58.52-60.59%) with the CoATs of *Lachnospiraceae* bacterium and *A. hadrus*. This may be because strain CPB6 belongs to the family *Ruminococcaceae*, which is closer to *Lachnospiraceae* and *Anaerostipes* at the taxonomic phylogeny level than *Megasphaera* and *Clostridium*.

Prediction and comparison of the three-dimensional (3D) structure and active site

As shown in Fig. 4*A*, the three-dimensional (3D) structure of CPB6-CoAT has one subunit which may consist of two main domains resulting in a characteristic two-domain fold in a homo-tetrameric structure. A comparison of the 3D structures of the six CoAT proteins (Fig. 4) showed that these CoATs shared similar conformations of the structural elements (α-helices and β-strands) with slight structural modifications in the loop regions and active centers, with the exception of the CoAT from *M. elsdenii* (Fig. 4*C*). The 3D structure of the *M. elsdenii* protein was obviously different from that of other CoATs, and the divergences were located not only in the structural elements of α-helices and β-strands but also in the loops. This may be attributed to the distant genetic relationship between *M. elsdenii* and the other five bacteria. Although *M. elsdenii* produces caproic acid via acetyl-CoA and succinate (34), the functions of the CoATs may differ between strain CPB6 and *M. elsdenii*. The 3D structures of CoATs among *C. tyrobutyricum* BEY8, *Lachnospiraceae* bacterium, and *A. hadrus* shared almost the same conformation of α-helices and β-strands except for some slight variation in the loops (Fig. 4*D–F*). The protein structure and active center structures between CPB6-CoAT and BEY8-CoAT were further compared, as shown in Fig. S4, and both showed similar 3D structures except for the location and structure of the active center. The predicted active sites of the six CoATs are shown in Table 4. The predicted active center of the CPB6-CoAT protein was located between amino acids 342 and 353 (GGQLDFVLGAYL) while the active center of the BEY8-CoAT protein (GGQIDFTRGASM) was located from amino acids 335 to 346, and both active site peptides contain a phenylalanine and tyrosine (Fig. S4).

The structure of proteins plays an important role in their functional properties and catalytic efficiency (35); for example, succinyl CoA:3-ketoate CoA transferase from pig heart (36) and 4-hydroxybutyrate CoA-transferase from *Clostridium aminobutyricum* (37) showed unexpected changes in protein modification and specific activity when their crystal structures changed. In this study, a comparison of the 3D and active center structures showed the similarities and differences between CPB6-CoAT and other CoATs (Fig. 4 and S4), which may have affected the enzyme

233 catalytic function and activity. On the basis of these results, it is of great significance to study the
234 functional differences caused by the structural changes in CoATs. The exact structure and function
235 of the active center of the CPB6-CoAT protein remains to be determined through subsequent
236 comprehensive experiments and analysis.

237

238 **Site-directed mutagenesis**

239 Site-directed mutagenesis was used to verify the active sites of the protein (38). According to the
240 predicted active center of CPB6-CoAT (GGQLDFVLGAYL, 342-353 aa), site-directed
241 mutagenesis targeting sites Asp346 and Ala351 was carried out to identify the effects of the two
242 residues on the catalytic activity of CPB6-CoAT. Specifically, Asp346 was replaced by His and
243 Ala351 was replaced by Pro via site-directed mutagenesis. The nucleotide substitutions were
244 confirmed by Sanger sequencing of the DNA (Fig. S5). Enzyme assays showed that compared to
245 wild-type CPB6-CoAT, the Asp346 substitution led to an approximately 76% loss of BCoAT
246 activity and 72% loss of CCoAT activity, while the Ala351 substitution resulted in an almost 50%
247 loss of BCoAT activity and 55% loss of CCoAT activity (Fig. 5). Moreover, as shown in Table 3,
248 the $k$cat/K_m values for butyryl-CoA and caproyl-CoA of the D346H mutant (1.734 and 5.663
249 $mM^{-1}min^{-1}$) and A351P mutant (4.797 and 12.75 $mM^{-1}min^{-1}$) were all lower than those of wild-
250 type CPB6-CoAT (10.82 and 41.08 $mM^{-1}min^{-1}$). This result indicated that the Asp346 and Ala351
251 residues play vital roles in the active center of CPB6-CoAT.

252 Notably, the exchange of Asp, an acidic amino acid, for His led to loss of a carboxy group and the
253 introduction of two amidogens. Similarly, the replacement of Ala with Pro led to loss of an
254 amidogen and the introduction of a carboxy group. Ala lacked a bulky side chain and therefore
255 would likely not have any steric and electrostatic effects, and this change would not destroy the
256 conformation of the main chain (39). Differences in structures and properties among the sequences

may be the reason for the differences in CoAT activity (40). These results demonstrated that the conserved motif (GGQLDFVLGAYL, 342-353 aa) of CPB6-CoAT is directly linked to enzymatic activity. In conclusion, the conserved motif was the catalytic center of CPB6-CoAT, within which the Asp346 and Ala351 residues were essential for CoAT activity. These findings provide significant information for further detailed research on the structures and functions of CPB6-CoAT.

Concluding remarks. In our present study, two CoA-transferase genes were identified by cloning and expression in *E. coli* BL21 (DE3) with the plasmid pET28a. CPB6-CoAT showed higher activity for caproyl-CoA than for butyryl-CoA, while BEY8-CoAT only had activity for butyryl-CoA. This result indicated that CPB6-CoAT is responsible for the final step of caproic acid production. The bioinformatics analysis revealed differences between CPB6-CoAT and other CoATs. Moreover, site-directed mutagenesis analysis demonstrated that the conserved motif (GGQLDFVLGAYL, 342-353 aa) was probably the active center of CPB6-CoAT, within which sites Asp346 and Ala351 residues were identified as critical residues that affect the enzymatic activity of CPB6-CoAT. These results confirmed the existence of a CCoAT involved in the production of caproic acid, and the enzyme is apparently different from the BCoAT responsible for the production of butyric acid. This study facilitates our understanding of the metabolism for chain elongation via the reverse β-oxidation pathway. However, the detailed CCoAT structure and its function in MCFA biosynthesis require further study through crystallization of proteins and X-ray crystal structure analysis.

Experimental Procedures

Strain growth conditions

E. coli DH5α (TsingKe, Chengdu, China) and *E. coli* BL21 (DE3) (Transgene, Beijing, China) were cultured in Luria broth (LB) medium supplemented with 50 μg/ml kanamycin (Sangon Biotech, Shanghai, China) at 37 ℃. *Ruminococcaceae* bacterium CPB6 was grown anaerobically at 37 ℃ in modified reinforced Clostridium medium (Binder, Qingdao, China) (20). *C. tyrobutyricum* BEY8 was grown anaerobically at 37 ℃ in TGY medium (30 g/L tryptone, 20 g/L glucose, 10 g/L yeast extract, and 1 g/L L-cysteine hydrochloric acid; pH 7.0).

Gene cloning and plasmid construction

The CoAT genes were amplified from the genomic DNA of *Ruminococcaceae* bacterium CPB6 (23) or *C. tyrobutyricum* BEY8 (24) through PCR using the primers listed in Table 1. During amplification, the following conditions were used: initial denaturation (5 min at 98 ℃), followed by 30 cycles of denaturation (10 s at 98 ℃), annealing (30 s at 52 ℃), and elongation (1 min at 72 ℃) and a final extension (5 min at 72 ℃). The PCR products were verified by agarose electrophoresis, recovered using a PCR purification kit (Fuji, Chengdu, China), and seamlessly inserted into the plasmid pET28a double digested with *Not* I and *Sal* I (Thermo, Waltham, USA) to construct the recombinant plasmid by using a seamless cloning kit (Biomed, Beijing, China). The recombinant plasmids were verified by Sanger sequencing and then transformed into *E. coli* BL21 (DE3) cells.

Expression and purification of the CoA-transferases

The recombinant plasmids pET28-CoAT-CPB6 (pET28-CCoAT) and pET28-CoAT-BEY8

(pET28-BCoAT) were transformed into *E. coli* BL21 (DE3). The transformed cells were cultured in LB medium containing 50 μg/ml kanamycin at 37 °C until the OD_{600} reached 0.5 and then further cultured at 22 °C for 12 h with 0.4 mM IPTG. The cultured cells were harvested by centrifugation (8,000 × *g*, 10 min) at 4 °C, and the cell pellet was resuspended in 50 mM potassium phosphate (pH 8.0). The cells were then disrupted by an ultrasonicator (Huxi, Shanghai, China) for 30 min (200 W, 4 s, interval 6 s) and centrifuged at 8,000 × *g* for 30 min to remove the insoluble material. Then, the enzyme was purified with Ni-NTA Sepharose (Genscript, Nanjing, China) and eluted with 50 mM sodium phosphate (pH 8.0) containing 300 mM NaCl and 250 mM imidazole. Finally, the purity and MW of the enzyme were assessed using SDS-PAGE analysis. Moreover, the enzyme was analyzed by western blotting with anti-6×His rabbit polyclonal antibody (Sangon Biotech, Shanghai, China). The protein concentrations were determined using a BCA protein assay kit (Solarbio, Beijing, China).

Enzymatic characterization

CoAT activity in crude enzyme extracts and of purified recombinant proteins was measured by determining the concentration of acetyl-CoA, a reaction byproduct, with the citrate synthase assay as described in previous studies with minor modifications (25,41). In brief, the reaction was initiated by the addition of enzyme (up to 20 ng/ml) and was performed in a total volume of 1.0 ml at 25 ℃: 100 mM potassium phosphate buffer (pH 7.0), 200 mM sodium acetate, 1.0 mM 5,5'-dithiobis (2-nitrobenzoate), 1.0 mM oxaloacetate, 8.4 *n*kat citrate synthase (Sigma, St. Louis, USA), 0.5 mM CoA derivatives (Sigma, St. Louis, USA). The released CoA, corresponding to the residual amount of acetyl-CoA, was detected by measuring the absorbance at 412 nm. One unit of activity is defined as the amount of enzyme which converts 1 μmol of acetyl-CoA per min under these conditions.

The kinetic parameters of the recombinant protein were also calculated by using the coupled spectrophotometric enzyme assay through citrate synthesis (16). The reaction mixture was the same as that mentioned above, and the concentrations of butyryl-CoA or caproyl-CoA were varied from 0.5 to 5 mM. The kinetic parameters were computed by using the Lineweaver–Burk transformation of the Michaelis-Menten equation, in which velocity is a function of the substrate (42,43). The catalytic constant (k_{cat}) was defined as the number of CoAT molecules formed by one molecule of enzyme in a single second. All measurements were performed in triplicate for biological replications.

Bioinformatics

Sequence alignment was performed using ESPript (44). Representative CoAT (8,45-47) sequences were downloaded from the NCBI database. MEGA-X software was used to perform sequence alignment and construct the phylogenetic tree (48). The active sites of CoATs were predicted by the online tool ScanProsite, and the three-dimensional CoAT structure was simulated by NCBI-CDD to search for templates in SWISS-MODEL and was embellished and labeled by PyMOL 2.3.3 software (49,50). The phylogenetic relationships of CoATs from different species were obtained by using OrthoFinder, the amino acid sequences were downloaded from the NCBI website (version 2.2.7) (51), and MUSCLE (v3.8.31) was used to calibrate the 119 shared single-copy genes (52). The phylogenomic tree was derived from a supermatrix comprising these shared single-copy genes with 41,213 unambiguously aligned amino acids using the maximum likelihood (43) method in RAxML (v8.2.10) (53) under the PROTGAMMAAUTO model, with 100 bootstrap replicates.

Site-directed mutagenesis

The point mutation vectors were constructed with the Fast Mutagenesis System (Transgene, Beijing, China). The QuikChange PCR method using pfu DNA polymerase was performed to generate the D346H mutant and A351P mutant. The recombinant plasmid (pET28a-CoAT-CPB6) was used as template DNA, and complementary mutagenic oligonucleotides as primers are shown in Table 1. After PCR amplification, the mixture was digested with restriction enzymes using D*pn*I to remove methylated template DNA and then sequenced (TsingKe, Chengdu, China) to verify site mutagenesis before being transformed into *E. coli* BL21 (DE3) (Transgene, Beijing, China). After purification, the enzymatic activities for butyryl-CoA and caproyl-CoA were measured following the method described above for the wild type.

Supplemental material

Supplemental material is available online only.

Acknowledgements

This work was supported by the Natural Science Foundation of China (31770090), the Open-foundation project of CAS Key Laboratory of Environmental and Applied Microbiology (KLCAS-2017-01). Additionally, we would like to thank Dr. Su Dan for her advice and assistance in this study.

Conflict of interest

The authors are aware of no conflict of interest.

References

1. Kenealy, W. R., Cao, Y. , Weimer, P. J. . (1995) Production of caproic acid by cocultures of ruminal cellulolytic bacteria and Clostridium kluyveri grown on cellulose and ethanol. *Applied Microbiology & Biotechnology* **44**, 507-513
2. Desbois, A. P. (2012) Potential applications of antimicrobial fatty acids in medicine, agriculture and other industries. *Recent patents on anti-infective drug discovery* **7**, 111-122
3. Herman, N. A., Li, J., Bedi, R., Turchi, B., Liu, X., Miller, M. J., and Zhang, W. (2017) Development of a High-Efficiency Transformation Method and Implementation of Rational Metabolic Engineering for the Industrial Butanol Hyperproducer Clostridium saccharoperbutylacetonicum Strain N1-4. *Appl Environ Microbiol* **83**, 02942-02916
4. Liu, B., Kleinsteuber, S., Centler, F., Harms, H., and Strauber, H. (2020) Competition Between Butyrate Fermenters and Chain-Elongating Bacteria Limits the Efficiency of Medium-Chain Carboxylate Production. *Front Microbiol* **11**, 1-13
5. Marounek M , F. K., Bartos S (1989) Metabolism and Some Characteristics of Ruminal Strains of Megasphaera elsdenii. *Appl Environ Microbiol* **55**, 1570-1573
6. Zhu, X., Tao, Y., Liang, C., Li, X., Wei, N., Zhang, W., Zhou, Y., Yang, Y., and Bo, T. (2015) The synthesis of n-caproate from lactate: a new efficient process for medium-chain carboxylates production. *Sci Rep* **5**, 14360-14369
7. Kucek L A , Nguyen M , and T, A. L. (2016) Conversion of L-lactate into n-caproate by a continuously fed reactor microbiome. *Water Research* **93**, 163-171
8. Wang, Y., Li, B., Dong, H., Huang, X., Chen, R., Chen, X., Yang, L., Peng, B., Xie, G., Cheng, W., Hao, B., Li, C., Xia, J., and Zhang, B. (2018) Complete Genome Sequence of Clostridium kluyveri JZZ Applied in Chinese Strong-Flavor Liquor Production. *Curr Microbiol* **75**, 1429-1433
9. Angenent, L. T., Richter, H., Buckel, W., Spirito, C. M., Steinbusch, K. J., Plugge, C. M.,

395 Strik, D. P., Grootscholten, T. I., Buisman, C. J., and Hamelers, H. V. (2016) Chain
396 Elongation with Reactor Microbiomes: Open-Culture Biotechnology To Produce
397 Biochemicals. *Environ Sci Technol* **50**, 2796-2810
398 10. Spirito, C. M., Richter, H., Rabaey, K., Stams, A. J., and Angenent, L. T. (2014) Chain
399 elongation in anaerobic reactor microbiomes to recover resources from waste. *Curr Opin*
400 *Biotechnol* **27**, 115-122
401 11. San-Valero, P., Abubackar, H. N., Veiga, M. C., and Kennes, C. (2020) Effect of pH, yeast
402 extract and inorganic carbon on chain elongation for hexanoic acid production. *Bioresour*
403 *Technol* **300**, 1-7
404 12. Scarborough, M. J., Myers, K. S., Donohue, T. J., and Noguera, D. R. (2020) Medium-
405 Chain Fatty Acid Synthesis by "Candidatus Weimeria bifida" gen. nov., sp. nov., and
406 "Candidatus Pseudoramibacter fermentans" sp. nov. *Appl Environ Microbiol* **86**, 1-19
407 13. Duncan, S. H., Barcenilla, A., Stewart, C. S., Pryde, S. E., and Flint, H. J. (2002) Acetate
408 utilization and butyryl coenzyme A (CoA):acetate-CoA transferase in butyrate-producing
409 bacteria from the human large intestine. *Appl Environ Microbiol* **68**, 5186-5190
410 14. Louis, P., and Flint, H. J. (2009) Diversity, metabolism and microbial ecology of butyrate-
411 producing bacteria from the human large intestine. *FEMS Microbiol Lett* **294**, 1-8
412 15. Yasuo Yoshida, Mitsunari Sato, Keiji Nagano, and Hasegawa, Y. (2015) Production of 4-
413 hydroxybutyrate from succinate semialdehyde in butyrate biosynthesis in Porphyromonas
414 gingivalis. *Biochimica Et Biophysica Acta General Subjects* **1850**, 2582-2591
415 16. Sato, M., Yoshida, Y., Nagano, K., Hasegawa, Y., Takebe, J., and Yoshimura, F. (2016)
416 Three CoA Transferases Involved in the Production of Short Chain Fatty Acids in
417 Porphyromonas gingivalis. *Front Microbiol* **7**, 1-13
418 17. Henning Seedorf, W. Florian Fricke, Birgit Veith, Holger Bru ggemann, H. L., Axel
419 Strittmatter, Marcus Miethke, Wolfgang Buckel, Julia Hinderberger, Fuli Li, Christoph

Hagemeier, Rudolf K. Thauer, and Gottschalk, G. (2008) The genome of Clostridium kluyveri, a strict anaerobe with unique metabolic features. *PNAS* **105**, 2128–2133

18. Heider, J. (2001) A new family of CoA-transferases. *FEBS* **509**, 345-349

19. Charrier, C., Duncan, G. J., Reid, M. D., Rucklidge, G. J., Henderson, D., Young, P., Russell, V. J., Aminov, R. I., Flint, H. J., and Louis, P. (2006) A novel class of CoA-transferase involved in short-chain fatty acid metabolism in butyrate-producing human colonic bacteria. *Microbiology* **152**, 179-185

20. Uwe Jacob, Matthias Mack, Tim Clausen, Robert Huber, Wolfgang Buckel, and Messerschmidt, A. (1996) Glutaconate CoA-transferase from Acidaminococcus fermentans the crystal structure reveals homology with other CoA-transferases. *Structure*, 415-426

21. Zhu, X., Zhou, Y., Wang, Y., Wu, T., Li, X., Li, D., and Tao, Y. (2017) Production of high-concentration n-caproic acid from lactate through fermentation using a newly isolated Ruminococcaceae bacterium CPB6. *Biotechnol Biofuels* **10**, 102-114

22. Wang, H., Li, X., Wang, Y., Tao, Y., Lu, S., Zhu, X., and Li, D. (2018) Improvement of n-caproic acid production with Ruminococcaceae bacterium CPB6: selection of electron acceptors and carbon sources and optimization of the culture medium. *Microb Cell Fact* **17**, 99-108

23. Yong Tao, Xiaoyu Zhu, Han Wang, Yi Wang, Xiangzhen Li, Hong Jin, and Rui, J. (2017) Complete genome sequence of Ruminococcaceae bacterium CPB6: A newly isolated culture for efficient n-caproic acid production from lactate. *Journal of Biotechnology* **259**, 91-94

24. Hu Xiaohong, Zhou Yan, Tao Yong, Zhu Xiaoyu, Liang Cheng, He Xiaohong, and Ping, G. (2016) Identification and Characterization of Clostridium BEY8 to Produce Butyrate from Lactate. *Journal of Sichuan University* **53**, 459-464

445 25. Scherf U, and W, B. (1991) Purification and properties of4-hydroxybutyrate coenzyme a
446 transferase from Clostridium aminobutyricum. *Appl Environ Microbiol* **57**, 2699-2702
447 26. González-Cabaleiro, R., Lema, J. M., Rodríguez, J., and Kleerebezem, R. (2013) Linking
448 thermodynamics and kinetics to assess pathway reversibility in anaerobic bioprocesses.
449 *Energy & Environmental Science* **6**, 3780-3789
450 27. D P Wiesenborn, F B Rudolph, and Papoutsakis, E. T. (1989) Coenzyme A Transferase
451 from Clostridium acetobutylicum ATCC 824 and Its Role in the Uptake of Acids. *Appl*
452 *Environ Microbiol* **55**, 323-329
453 28. Lee, J., Jang, Y. S., Han, M. J., Kim, J. Y., and Lee, S. Y. (2016) Deciphering Clostridium
454 tyrobutyricum Metabolism Based on the Whole-Genome Sequence and Proteome Analyses.
455 *mBio* **7**, 1-12
456 29. Louis, P., Young, P., Holtrop, G., and Flint, H. J. (2010) Diversity of human colonic
457 butyrate-producing bacteria revealed by analysis of the butyryl-CoA:acetate CoA-
458 transferase gene. *Environ Microbiol* **12**, 304-314
459 30. Li, T. B., Zhao, F. J., Liu, Z., Jin, Y., Liu, Y., Pei, X. Q., Zhang, Z. G., Wang, G., and Wu,
460 Z. L. (2019) Structure-guided engineering of ChKRED20 from Chryseobacterium sp.
461 CA49 for asymmetric reduction of aryl ketoesters. *Enzyme Microb Technol* **125**, 29-36
462 31. Makabe, K., Hirota, R., Shiono, Y., Tanaka, Y., and Koseki, T. (2020) Biochemical and
463 structural investigation of rutinosidase from Aspergillus oryzae. *Appl Environ Microbiol*
464 32. Bilen, M., Mbogning, M. D., Cadoret, F., Dubourg, G., Daoud, Z., Fournier, P. E., and
465 Raoult, D. (2017) 'Pygmaiobacter massiliensis' sp. nov., a new bacterium isolated from the
466 human gut of a Pygmy woman. *New Microbes New Infect* **16**, 37-38
467 33. Sitkin, S., and Pokrotnieks, J. (2019) Clinical Potential of Anti-inflammatory Effects of
468 Faecalibacterium prausnitzii and Butyrate in Inflammatory Bowel Disease. *Inflamm Bowel*
469 *Dis* **25**, e40-e41

34. Lee, N. R., Lee, C. H., Lee, D. Y., and Park, J. B. (2020) Genome-Scale Metabolic Network Reconstruction and In Silico Analysis of Hexanoic acid Producing Megasphaera elsdenii. *Microorganisms* **8**

35. Zoraghi, R., See, R. H., Gong, H., Lian, T., Swayze, R., Finlay, B. B., Brunham, R. C., McMaster, W. R., and Reiner, N. E. (2010) Functional analysis, overexpression, and kinetic characterization of pyruvate kinase from methicillin-resistant Staphylococcus aureus. *Biochemistry* **49**, 7733-7747

36. Stephanie D. Tammam, Jean-Christophe Rochet, and Fraser, M. E. (2007) Identification of the Cysteine Residue Exposed by the Conformational Change in Pig Heart Succinyl-CoA:3-Ketoacid Coenzyme A Transferase on Binding Coenzyme A. *Biochemistry* **46**, 10852-10863

37. Macieira, S., Zhang, J., Velarde, M., Buckel, W., and Messerschmidt, A. (2009) Crystal structure of 4-hydroxybutyrate CoA-transferase from Clostridium aminobutyricum. *Biol Chem* **390**, 1251-1263

38. Thorsten Selmer, Angela Willanzheimer, and Hetzel, M. (2002) Propionate CoA-transferase from Clostridium propionicum: Cloning of the gene and identification of glutamate 324 at the active site. *Eur. J. Biochem.* **269**, 372-380

39. Cao, J., Dang, G., Li, H., Li, T., Yue, Z., Li, N., Liu, Y., Liu, S., and Chen, L. (2015) Identification and Characterization of Lipase Activity and Immunogenicity of LipL from Mycobacterium tuberculosis. *PLoS One* **10**, e0138151

40. Park, S. H., Kim, S. J., Park, S., and Kim, H. K. (2019) Characterization of Organic Solvent-Tolerant Lipolytic Enzyme from Marinobacter lipolyticus Isolated from the Antarctic Ocean. *Appl Biochem Biotechnol* **187**, 1046-1060

41. Lindenkamp, N., Schurmann, M., and Steinbuchel, A. (2013) A propionate CoA-transferase of Ralstonia eutropha H16 with broad substrate specificity catalyzing the CoA

thioester formation of various carboxylic acids. *Appl Microbiol Biotechnol* **97**, 7699-7709

42. Bloess, S., Beuel, T., Kruger, T., Sewald, N., Dierks, T., and Fischer von Mollard, G. (2019) Expression, characterization, and site-specific covalent immobilization of an L-amino acid oxidase from the fungus Hebeloma cylindrosporum. *Appl Microbiol Biotechnol* **103**, 2229-2241

43. Buckel W, Dorn U, and R, S. (1981) Glutaconate CoA-Transferase from Acidaminococcus fermentans. *Eur. J. Biochem.* **118**, 315–321

44. Cuff, J. A., and Barton, G. J. (2000) Application of multiple sequence alignment profiles to improve protein secondary structure prediction. *Proteins* **40**, 502-511

45. Dowd, S. E., Callaway, T. R., Wolcott, R. D., Sun, Y., McKeehan, T., Hagevoort, R. G., and Edrington, T. S. (2008) Evaluation of the bacterial diversity in the feces of cattle using 16S rDNA bacterial tag-encoded FLX amplicon pyrosequencing (bTEFAP). *BMC Microbiol* **8**, 1-8

46. Bajaj, J. S., Ridlon, J. M., Hylemon, P. B., Thacker, L. R., Heuman, D. M., Smith, S., Sikaroodi, M., and Gillevet, P. M. (2012) Linkage of gut microbiome with cognition in hepatic encephalopathy. *Am J Physiol Gastrointest Liver Physiol* **302**, G168-175

47. Kant, R., Rasinkangas, P., Satokari, R., Pietila, T. E., and Palva, A. (2015) Genome Sequence of the Butyrate-Producing Anaerobic Bacterium Anaerostipes hadrus PEL 85. *Genome Announc* **3**, 1-2

48. Tamura, K., Peterson, D., Peterson, N., Stecher, G., Nei, M., and Kumar, S. (2011) MEGA5: molecular evolutionary genetics analysis using maximum likelihood, evolutionary distance, and maximum parsimony methods. *Mol Biol Evol* **28**, 2731-2739

49. Arnold, K., Bordoli, L., Kopp, J., and Schwede, T. (2006) The SWISS-MODEL workspace: a web-based environment for protein structure homology modelling. *Bioinformatics* **22**, 195-201

50. Marchler-Bauer, A., Anderson, J. B., Chitsaz, F., Derbyshire, M. K., DeWeese-Scott, C., Fong, J. H., Geer, L. Y., Geer, R. C., Gonzales, N. R., Gwadz, M., He, S., Hurwitz, D. I., Jackson, J. D., Ke, Z., Lanczycki, C. J., Liebert, C. A., Liu, C., Lu, F., Lu, S., Marchler, G. H., Mullokandov, M., Song, J. S., Tasneem, A., Thanki, N., Yamashita, R. A., Zhang, D., Zhang, N., and Bryant, S. H. (2009) CDD: specific functional annotation with the Conserved Domain Database. *Nucleic Acids Res* **37**, D205-210

51. Emms, D. M., and Kelly, S. (2015) OrthoFinder: solving fundamental biases in whole genome comparisons dramatically improves orthogroup inference accuracy. *Genome Biol* **16**, 1-14

52. Edgar, R. C. (2004) MUSCLE: multiple sequence alignment with high accuracy and high throughput. *Nucleic Acids Res* **32**, 1792-1797

53. Stamatakis, A. (2014) RAxML version 8: a tool for phylogenetic analysis and post-analysis of large phylogenies. *Bioinformatics* **30**, 1312-1313

Tables

Table 1. Bacterial strains, plasmids, and primers used in this study.

	Description	Reference or source
Strains		
CPB6	*Ruminococcaceae* bacterium CPB6	Zhu XY et al.(21)
BEY8	*Clostridium tyrobutyricum* BEY8	Hu XH et al.(24)
E. coli DH5α	TreliefTtMm 5α Chemically Competent Cell	TsingKe
E. coli BL21 (DE3)	Expression Chemically Competent Cell	Transgene
Plasmids		
pET28a	*E. coli* expression vector (Kan, T7 promoter)	This study
pET28a-CoAT-CPB6	pET28a carrying gene CoAT from CPB6 fused with His tag in N-terminus	This study
pET28a-CoAT-BEY8	pET28a carrying gene CoAT from BEY8 fused with His tag in N-terminus	This study
D346H-mutant	The 346 aa Asp mutation of CoAT in pET28a-CoAT-CPB6	This study
A351P-mutant	The 351 aa Ala mutation of CoAT in pET28a-CoAT-CPB6	This study
Primers	Sequence (5′-3′)	
YT43-SalI-fw	TAATACGACTCACTATAGGG	This study
YT44-NotI-rv	GCTAGTTATTGCTCAGCGG	This study
YT50-CPB6-fw[a]	GTGGTGCTCGAGTGCATGAGTTTTCAAGAAGAATATGCACAAA AACTGAC	This study
YT51-CPB6-rv[a]	CGAATTCGAGCTCCGTTAAATTTTATTGCTTCTGCGCCAGATGC	This study
YT52-BEY8-fw[a]	CGAATTCGAGCTCCGTCGACATGAGTTTTGAGGAATTGTATAAG AGTAAAGTTGTTAGT	This study
YT53-BEY8-rv[a]	GTGGTGCTCGAGTGCGGCCGCTTTTATAAGTTCTCTAGCTCTTT GTTTTAATGTCTTACCTCTAAG	This study
YT60-A351P-fw[b]	AGCTGGATTTTGTTCTGGGT**C**CCTATCTGAGCCACGGT	This study
YT61-A351P-rv[b]	**G**ACCCAGAACAAAATCCAGCTGACCGGCAC	This study
YT62-D346H-fw[b]	AGCGGTGCCGGTGGTCAGCTG**C**ATTTTGTTCT	This study
YT63-D346H-rv[b]	**G**CAGCTGACCACCGGCACCGCTAATCTGACGAAA	This study

[a] Underscored letters match the sequence of vectors for seamless cloning.

[b] The sequences corresponding to the mutated codons are written in bold.

Table 2. Purification and specific activities of the CoATs[a]

Enzyme	Total protein, mg	Total activity, U	Specific activity, U/mg of protein		Purification fold
			Butyryl-CoA	Caproyl-CoA	
The CPB6-CoAT					
Crude extract	87.04	180.2	2.07±0.06	5.11±0.08	1
Purified protein[b]	22.61	244.2	10.8±0.02	27.6±0.15	5.4
The BEY8-CoAT					
Crude extract	63.10	436.0	6.91±0.12	ND[a]	1
Purified protein[b]	17.66	462.7	26.2±0.09	ND[a]	3.8

[a] The purification data in the table were from 300 ml of culture medium. U = μmol/min. ND = not detectable.

[b] Protein was purified with affinity chromatography.

544 **Table 3. Kinetic parameters for the CoATs.**

Enzyme	Butyryl-CoA				Caproyl-CoA				Reference
	K_m (μM)	k_{cat} (min^{-1})	k_{cat}/K_m ($mM^{-1}min^{-1}$)	V_m (μM min^{-1})	K_m (μM)	k_{cat} (min^{-1})	k_{cat}/K_m ($mM^{-1}min^{-1}$)	V_m (μM min^{-1})	
BEY8-CoAT	369.5	13.91	37.65	27.81	ND[c]	ND[c]	ND[c]	ND[c]	This study
CPB6-CoAT	536.9	5.810	10.82	11.62	358.8	14.74	41.08	29.51	This study
CPB6-CoAT-D346H-mutant	747.4	1.296	1.734	2.592	747.8	4.235	5.663	8.469	This study
CPB6-CoAT-A351P-mutant	622.7	2.987	4.797	5.975	532.1	6.784	12.75	13.57	This study
PGN_0725[a]	520.0	9.33	17.95	71.51	NR[c]	NR[c]	NR[c]	NR[c]	Sato, Yoshida et al. 2016 (16)
CoA transferase[b]	21.01	NR[c]	NR[c]	NR[c]	NR[c]	NR[c]	NR[c]	NR[c]	Papoutsakis. 1989 (27)

545 [a] Butyryl-CoA:acetate CoA transferase from *Porphyromonas gingivalis*.

546 [b] Butyryl-CoA:acetate CoA transferase from *Clostridium acetobutylicum* ATCC 824.

547 [c] ND is defined as not determined; NR, not reported.

548

549 **Table 4. Prediction of the active sites of CoATs in different strains.**

Strain	Location of active site	Sequence of active site
Ruminococcaceae bacterium CPB6 (ARP50528.1)	342-353	GGQLDFVLGAYL
Clostridium kluyveri (APM41307.1)	335-346	GGQVDFIRGANL
Megasphaera elsdenii (WP_036202574.1)	356-367	ADSYTYKKAPTL
Clostridium tyrobutyricum BEY8 (WP_017752740.1)	335-346	GGQIDFTRGASM
Lachnospiraceae bacterium (HCI66479.1)	340-351	GGQLDFVLGAYK
Anaerostipeshadrus(WP_044923342.1)	342-353	GGQLDFVMGAYL

550

551

552 **Figure captions**

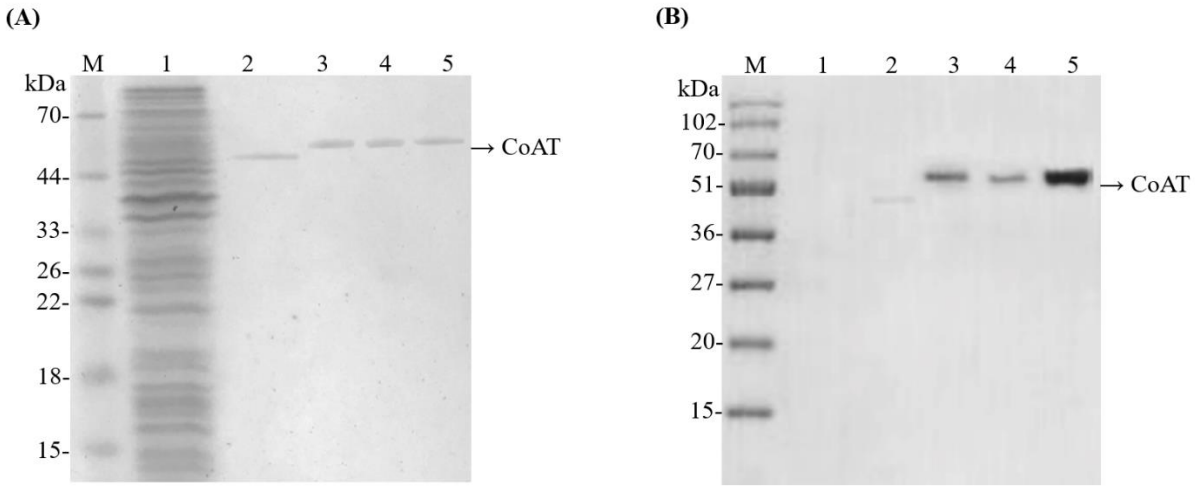

553

554 **FIGURE 1. Purification and western blot analysis of CPB6-CoAT (CCoAT) and BEY8-CoAT**

555 **(BCoAT).** Analysis of the purified CCoAT and BCoAT by SDS-PAGE **(A)**. Analysis of the purified

556 CCoAT and BCoAT by western blotting with anti-His-tag antibody **(B)**. M, molecular mass marker.

557 Lanes: 1, pET28a; 2, BCoAT; 3, CCoAT; 4, CCoAT-D346H mutant; 5, CCoAT-A351P mutant.

558 Samples (~2 μg) were visualized by Coomassie Brilliant Blue staining after electrophoresis.

559 Molecular mass positions are shown by markers (kDa).

560

561

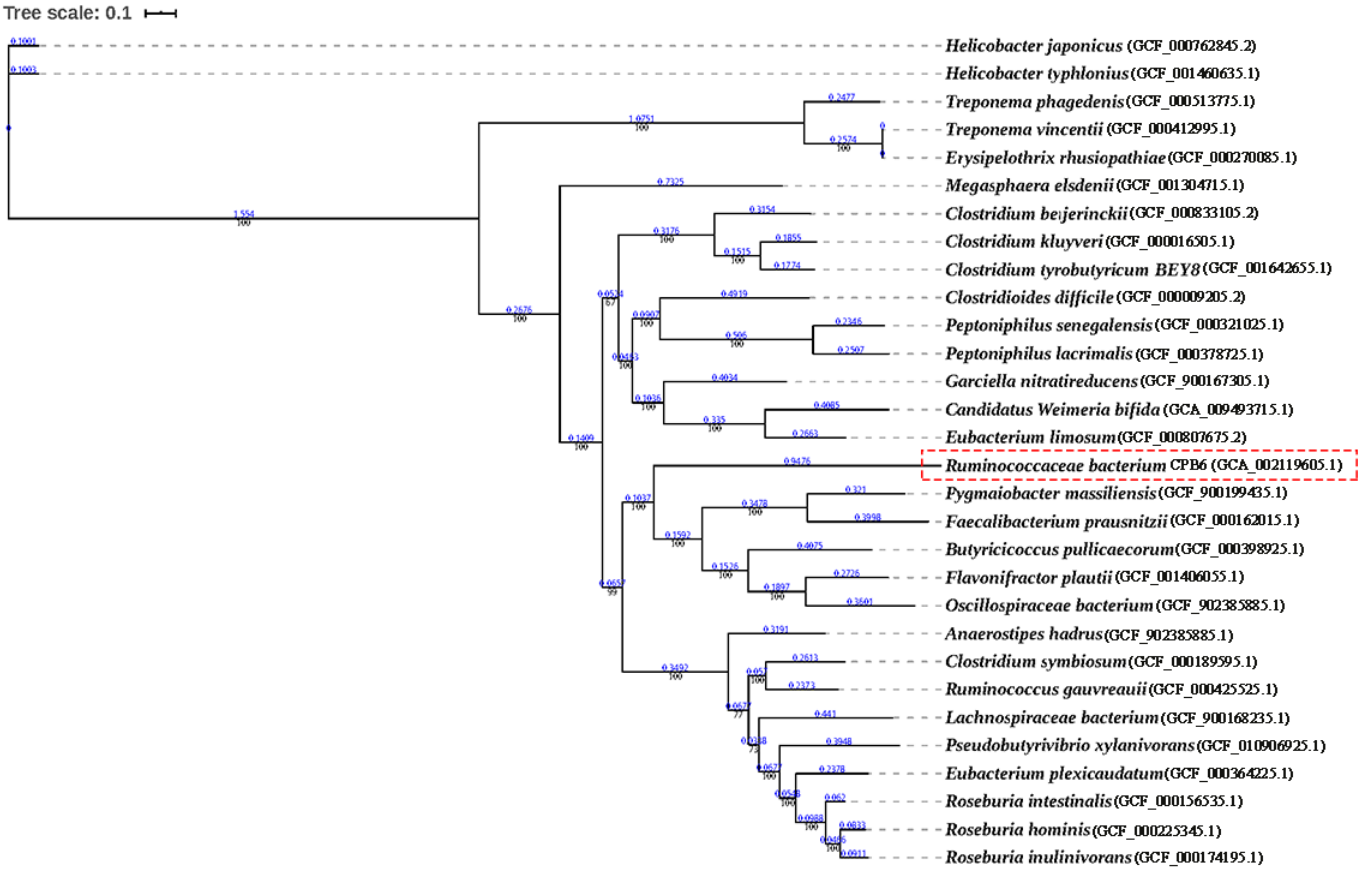

562 **FIGURE 2. Phylogenetic tree of the whole genomes of 29 strains containing the CoA-**
563 **transferase.** Numbers at the nodes indicate the levels of bootstrap values. The scale bar for the tree
564 represents a distance of 0.1 substitutions per site.

565

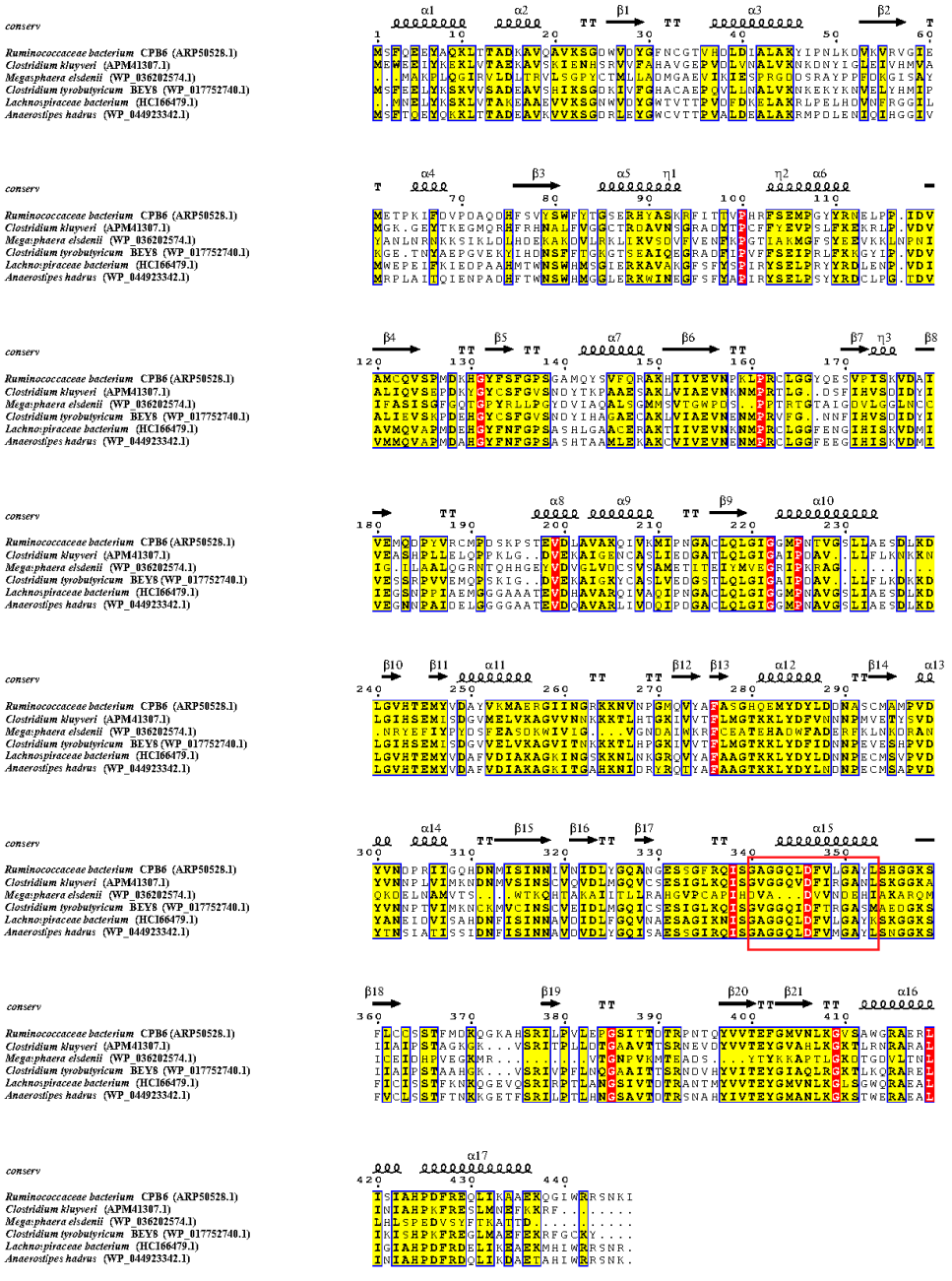

FIGURE 3. Multiple amino acid sequence alignment for CoATs. There were 17 α-helices and 21 β-pleated sheets, which are represented with symbols. Nonconserved, 60% conserved, and 100% conserved residues are marked with white, yellow, and red font, respectively. Conserved motifs are boxed with a red frame.

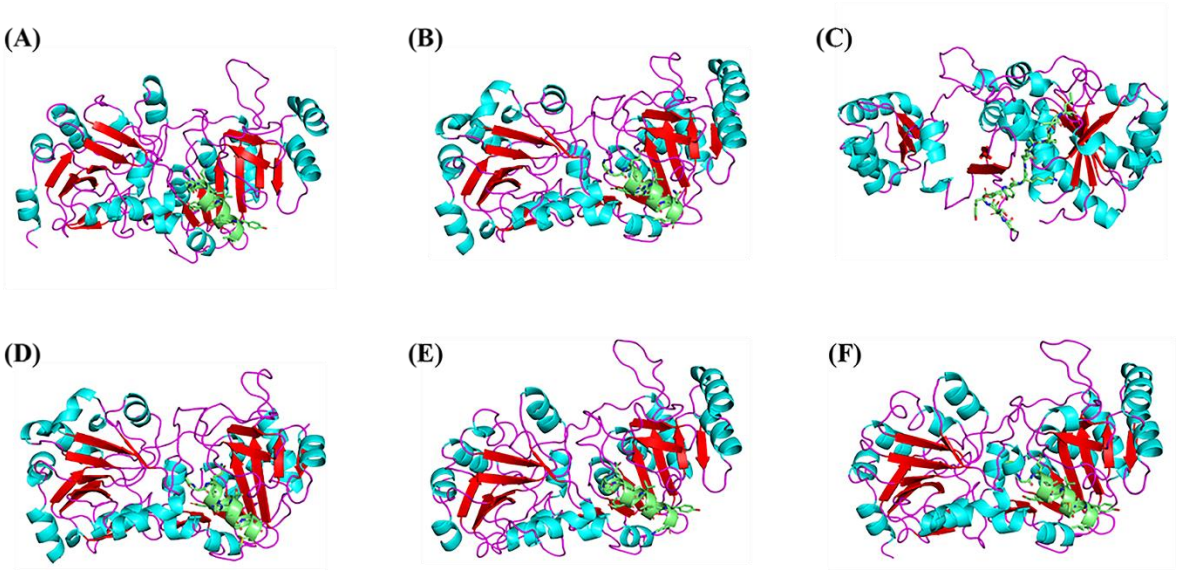

572

573 **FIGURE 4. Predicted 3D structures of representative CoAT proteins.** 3D structures of CoATs
574 from *Ruminococcaceae* bacterium CPB6 **(A)**, *Clostridium kluyveri* **(B)**, *Megasphaera elsdenii* **(C)**,
575 *Clostridium tyrobutyricum* BEY8 **(D)**, *Lachnospiraceae* bacterium **(E)**, and *Anaerostipes hadrus*
576 **(F)**. Helices of the catalytic domains, β-pleated sheets, loop regions, and active centers are colored
577 sky blue, red, purple, and green, respectively.

578

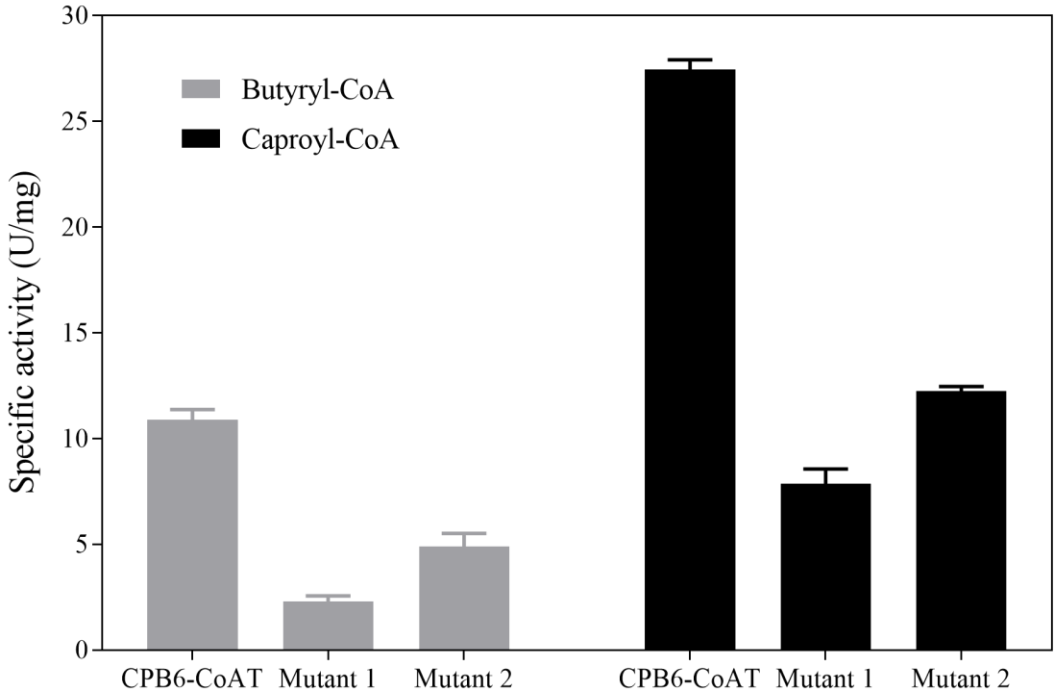

579

580 **FIGURE 5. Comparison of CoA-transferase activities** (Mutant 1, D346H-mutant; Mutant 2,
581 A351P-mutant). The specific activity with butyryl-CoA as the substrate is labeled in light gray, and
582 the specific activity with caproyl-CoA as the substrate is marked in dark gray. The values represent
583 the means ± SDs of three independent experiments.